JOURNAL OF AGRICULTURAL AND FOOD CHEMISTRY

Food and Beverage Chemistry/Biochemistry

Oxidation of procyanidins with various degrees of condensation: influence on the color deepening phenomenon

Yoshihide Hibi, and Emiko Yanase

J. Agric. Food Chem., **Just Accepted Manuscript** • DOI: 10.1021/acs.jafc.9b02085 • Publication Date (Web): 16 Apr 2019

ACS Publications

is published by the American Chemical Society. 1155 Sixteenth Street N.W., Washington, DC 20036

Oxidation of procyanidins with various degrees of condensation: influence on the color deepening phenomenon

Yoshihide Hibi, Emiko Yanase*

Faculty of Applied Biological Sciences, Gifu University, 1-1 Yanagido, Gifu 501-1193, Japan

*Corresponding author:

Emiko Yanase

TEL/FAX +08-58-293-2914

E-mail e-yanase@gifu-u.ac.jp

ABSTRACT

Color deepening in red rice is a known phenomenon that occurs during post-harvest storage. As procyanidins potentially causes this color deepening, we previously subjected synthetic procyanidin B3, a model procyanidin, to chemical oxidation and determined the structures of the products. To further elucidate the effects of various degrees of polymerization on color deepening, in this study we oxidized synthetic procyanidin C2. The intensity of the UV-Vis absorption between 300 and 500 nm in the spectrum of the reaction mixture increased with increasing oxidation time. This absorption following the oxidation of procyanidin C2 was more intense than that of procyanidin B3. HPLC-ESI-MS of the oxidized reaction mixture revealed several new peaks that suggested the formation of products with new intramolecular rather than intermolecular bonds. The major product was structurally identified by comparison with the UPLC-ESI-MS/MS data for a synthetic procyanidin C2 oxide, independently prepared by condensing procyanidin B3 oxide and taxifolin.

KEYWORDS: Color deepening, polymerization degree, catechin, procyanidin, HPLC-ESI-MS

INTRODUCTION

Many varieties of rice (*Oryza sativa*) are cultivated around the world, and those with pigments are commonly known as colored rice varieties. Almost all pigments are contained within the bran layers, and colored rice is classified as red or black based on its color. The main pigment in black rice is anthocyanin. Although the pigment of red rice has been presumed to be an anthocyanin, it is not observed in its extract; hence, the major pigment has not yet been clearly identified.

Procyanidin is present in the bran layers of red rice. It is condensed tannin composed of flavan-3-ol units, such as catechin, epicatechin, gallocatechin, and epigallocatechin, which are widely distributed in plants, particularly in fruits. They are classified into two types (A and B) according to their bonding systems. These bioactive constituents exhibit beneficial biological properties, including strong anti-oxidative, anti-inflammatory, and anti-cancer activities.[1-4] The color of red rice intensifies during ripening after flowering, and becomes darker in the post-harvest storage period. This phenomenon is the result of chemical changes undergone by the preexisting components of the red rice; however, the detailed mechanism associated with these changes is not clear. We presume that color-deepening is related to the oxidation of the procyanidins in the red rice and previously studied the oxidation of procyanidin B3, a model

procyanidin, and isolated several novel oxidized products with spiro-type skeletons that contain new internal bonds.[5,6]

The procyanidins present in red rice are generally assumed to have polymeric structures that range from 2-mers to 14-mers, depending on the cultivar. Therefore, it is difficult to explain the color-deepening phenomenon from the knowledge gained through the oxidation of the model procyanidin B3 alone. In order to elucidate the effects of the degree of catechin polymerization on the oxidation reaction and the color change, in this study we synthesized procyanidin C2, as a model procyanidin, and subjected it to chemical oxidation.

MATERIALS AND METHODS

Chemicals (+)-Catechin (**1**) was purchased from Sigma-Aldrich Co. (St. Louis, MO, USA) and (+)-taxifolin (**2**) was isolated and purified from larch.[7] Copper(II) chloride dihydrate ($CuCl_2 \cdot 2H_2O$), 2-mercaptoethanol, and all solvents were purchased from Nacalai Tesque Co. (Kyoto, Japan).

Instrumentation Column chromatography was performed on Diaion HP20SS resin (Mitsubishi Chemical Co., Tokyo, Japan). HPLC was performed using a

JASCO PU2089 intelligent pump equipped with a JASCO MD-2010 detector and a JASCO CO-2065 column oven (Tokyo, Japan).

Preparation of the red rice procyanidin fraction. Red rice (20 g) was soaked for 6 h in water (70 mL) at room temperature. After filtration, the solid was extracted for 1 day with acetone (50 mL) at room temperature. After removal of the solid by filtration, the acetone was removed by rotary evaporation and the extract was subjected to column chromatography. To obtain the procyanidin rich fraction, fractionation was performed using a Diaion HP20SS column (20 mm I.D. × 200 mm). The extract reside was dissolved in water and then adsorbed on the column. The sample was eluted sequentially with 0%, 20%, and 50% aqueous MeOH. The fraction that eluted with 50% aqueous MeOH was evaporated under reduced pressure to leave a residue (100.3 mg). The sample was subjected to HPLC with a HILIC column (Inertsil Amide 4.6 mm I.D. × 250 mm). The column temperature was maintained at 35°C. The mobile phase consisted of H_2O (A) and MeCN (B) at a flow rate of 1.0 mL/min. The following linear gradient was used for analysis: 85% to 65% B over 15 min.

Synthesis of procyanidin C2 (4). Procyanidin B3 was prepared from catechin and taxifolin following a literature procedure.[6,8] (+)-Taxifolin (**2**, 50 mg) was dissolved in EtOH (1.0 mL). Sodium borohydride (75 mg) was added under argon and

stirred 30min. Water (10 mL) was added to the mixture to decompose the excess sodium borohydride, and the pH was adjusted to below 5.0 with acetic acid. Procyanidin B3 (**3**, 200 mg) in 50% aqueous EtOH was then added to the mixture at 40°C and stirred for 3 h.[8] The reaction mixture was extracted with ethyl acetate and concentrated. The ethyl acetate extract was purified by HPLC using a HILIC column (Inertsil Amide 10 mm I.D. × 250 mm, 5 μm (GL Sciences Inc., Tokyo, Japan)). The mobile phase consisted of 90% MeCN in H_2O, at a flow rate of 5.0 mL/min, and an injection volume of 50 μL. Procyanidin C2 (**4**, 41 mg, purity > 95% by HPLC) was obtained in this manner. The chemical structure of **4** was confirmed by comparing its NMR and MS data with those in the literature.[8] The structures of catechin (**1**), taxifolin (**2**), procyanidin B3 (**3**), procyanidin C2 (**4**), and oxidative procyanidin B3 (**5**) are shown in Fig. 1.

Oxidation of 4 and the procyanidin fraction of red rice. An aqueous solution of **4** (2.0 mg) and $CuCl_2 \cdot 2H_2O$ (6.0 mg) was vigorously stirred at room temperature. An aliquot of the reaction mixture at each reaction period (0.5, 1, 2, and 4 h) was subjected to Diaion HP20SS column chromatography. After washing with water to remove $CuCl_2 \cdot 2H_2O$, the column was eluted with MeOH. Each MeOH fraction was concentrated and the residue (2.1 mg) examined by reverse-phase HPLC (NB-ODS-9

4.6 mm I.D. × 250 mm). The column temperature was maintained at 35°C. The mobile phase consisted of 10% MeCN / 0.5% HCOOH in H_2O, at a flow rate of 1.0 mL/min. An injection volume of 10 μL was used.

UV-Vis spectroscopy. The mixtures of oxidation products were dissolved in MeOH to a concentration of 0.10 g/L. UV/Vis spectra were recorded on a Perkin Elmer Lambda 950 UV/VIS/NIR spectrophotometer (Kanagawa, Japan). The spectrum of each sample was acquired in the 200–600 nm wavelength range at a spectral resolution of 1 nm. The spectra were recorded against the corresponding solvent as the baseline.

Thiolysis of the mixture obtained by the oxidation of 4. Thiolysis was conducted according to the procedure reported by Tanaka et al., with slight modifications.[9] The oxidation-product mixture containing the trimer (1 mg) was dissolved in EtOH (1.6 μL), and 0.2 N aqueous HCl (1.6 μL) and 2-mercaptoethanol (2.0 μL) were added; the mixture was then stirred at room temperature for 24 h, after which the EtOH was removed under reduced pressure. The aqueous solution was separated by Diaion HP20SS column chromatography and monitored by HPLC with a HILIC column (Inertsil Amide 4.6 mm I.D. × 250 mm). The column temperature was maintained at 35°C. The mobile phase consisted of 90% MeCN in H_2O at a flow rate of 1.0 mL/min; the injection volume was 10 μL.

UPLC-ESI-MS. Ultra-high-performance liquid chromatography–time-of-flight mass spectrometry (UPLC-TOF-MS) was performed using a Waters Xevo G2 QTof (Waters, USA) mass spectrometer, equipped with a C18 analytical column (ACQUITY UPLC BEH C_{18} 2.1 mm I.D. × 100 mm; Waters, USA) and a HILIC column (Inert Sustain Amide HP 3 μm, 2.1 mm I.D. × 150 mm; GL Science, Japan). The mobile phase consisted of 1.0% HCOOH in H_2O (A) and MeCN (B), with a flow rate of 0.2 mL/min and an injection volume of 1.0 μL used. The column temperature was maintained at 35°C. The mobile phase for analysis of the trimer oxidation products was 10% B for 20 min for the C18 analytical column, or 90% B for 30 min for the HILIC column. The following linear gradient was used to analyze the thiolysis reaction mixture: 90% to 85% B for 15 min using the HILIC column. The ESI interface was operated in negative mode. MS parameters for analysis were: capillary potential, 2.5 kV; sampling cone, 30 V for in-source collision-induced dissociation (CID); desolvation temperature, 500°C; and source temperature, 150°C. The mass spectrometer was operated in MS/MS mode with a collision cell energy of 25 V for the oxide of **4**.

RESULTS AND DISCUSSION

UV/Vis Spectra Measurements. The UV-Vis spectra of the oxidation

mixtures of both **3** and **4** were acquired in order to study the relationship between chemical structure and color. The absorption band between 300 and 500 nm for each sample was more intense following oxidation (Figs. 2-A and B). The relationship between the absorbance at 330 nm of each sample and time is shown in Fig. 2-C. The increase in the absorbance at 330 nm following oxidation was four times greater for **4** than that it was for **3**. In addition, although moderate changes in absorption were observed for the reaction mixture of **3** beyond ~1 h, **4** exhibited an absorption that continued to increase even after 2 h.

The procyanidin fraction of the red rice extract was next subjected to oxidation for 2 h and examined by UV-Vis spectroscopy (Fig. S2). 2-Mer-to-8-mer procyanidins were observed in this sample by HPLC (Fig. S3), with the intensity of the absorption band in the 300–500 nm range observed to increase, in addition to the absorption maximum near 280 nm. This trend is similar to that observed for the oxidations of **3** and **4**; therefore, we assume that the oxidation systems in this study, namely **3** and **4**, are good models for assessing the effects of procyanidin oxidation on color change. Moreover, we assume that the degree of procyanidin polymerization significantly influences the color-deepening phenomenon.

HPLC. The oxidized mixtures of **3** and **4** were subjected to HPLC. The

143 time-dependent decreases in the contents of **3** and **4** under oxidative conditions are
144 shown in Figs. S4 and S5. The contents of both model compounds **3** and **4** decrease
145 sharply after commencement of oxidation. Trimer **4** was observed to react faster than
146 dimer **3**, and required only 1 h to disappear completely from the mixture (Fig. 3).
147 The major oxidation products of **3** appear to be spiro-type compounds, as
148 represented by compound **5**, among others, (Figs. 1 and S1) and have been reported
149 previously.[6] In contrast, a complicated assortment of peaks (**a**–**k**) was observed in the
150 HPLC trace following the oxidation of **4**; reactions continued following the
151 disappearance of compound **4**, as evidenced by changes in the intensities of these peaks
152 (Figs. S4 and S5). Several peaks (e.g., peak **j**) were observed to increase in intensity,
153 whereas others (e.g., peak **k**) decreased. The UV-Vis spectra of the fractions
154 corresponding to peaks **a**–**k** were acquired using an HPLC-photodiode array (PDA)
155 detector (Fig. S6). Although the maximum absorption wavelengths of these fractions
156 were similar to that of compound **4**, the ratios of the absorption intensities in the 300–
157 400 nm region to the that of maximum absorption peak were higher, suggesting that
158 these peaks correspond to oxidation products involved in the color deepening process.
159 **UPLC-MS.** The mixture resulting from the oxidation from **4** was subjected to
160 UPLC-MS. Molecular ion peaks were observed at *m/z* 861 or 863 $[M-H]^-$, although a

161 variety of new peaks were observed by HPLC (Figs. 4, S7, and S8). These data suggest
162 that the oxidation products contain new intramolecular bonds rather than intermolecular
163 bonds, which is similar to the trend observed for the oxidation of **3**. UPLC-MS traces
164 for each reaction period are shown in Figs. 4 and S7. Many complex overlapping peaks
165 are observed in the total ion chromatograms (TICs) and the chromatograms at 280 nm.
166 The reconstructed ion chromatograms for *m/z* 863 and 861 facilitated the resolution of
167 multiple well-separated peaks with the same mass number that correspond to positional-
168 or stereo-isomers. De Taeye et al. reported that Procyanidin is chemically modified by
169 food processes;[10, 11] in their research, procyanidin B2 and C1, which are the dimer and
170 trimer of epicatechin, were epimerized by heating in a model aqueous system, to
171 generate dehydrodicatechin A; however, this was not observed in our experiment. It is
172 well known that catechin rapidly epimerizes at the 2-position at high temperatures in an
173 aqueous medium.[12] In addition, De Taeye et al.[10] concluded that dehydrodicatechin A[13-
174 16] is formed from procyanidin B2 only at high temperatures because cleavage of the
175 interflavan linkage is required in order to generate the catechin monomer. Because our
176 oxidation experiments were performed at room temperature, we believe that
177 procyanidin C2 does not epimerize to generate a dehydrodicatechin A-like component.
178 We conclude that many peaks are observed because several potential positions for

179 reaction exist in the trimer molecule. In addition, we assume that the trimer oxide
180 epimerizes during the reaction. In fact, three isomers of the dimer oxide **5** were
181 observed in the reaction solution following the oxidation of **3** (Fig. S1).[6] Many large
182 peaks are observed in the initial stages of the reconstructed *m/z* 863 ion chromatogram,
183 which is 2 Da smaller than the *m/z* value of **4**; these peaks decrease in size with
184 increasing reaction time. In addition, the intensities of the peaks corresponding to *m/z*
185 861, which is 4 Da smaller than that of **4**, increase as the reaction progresses. These
186 results suggest that the oxidation process involves multiple steps rather than a single
187 step.

188 **UPLC-MS/MS.** Almost all of the peaks observed by UPLC-MS following
189 the oxidation of **4** were observed to have *m/z* 861 $[M-H]^-$ or 863 $[M-H]^-$ peaks (Fig.
190 S7); hence, each peak was subjected to MS/MS analysis (Fig. S9). MS/MS of the *m/z*
191 863 peak, with a retention time of 15.9 min, produced fragment ion peaks at *m/z* 287,
192 407, 449, 455, 575, 693, 711, and 737. The fragments at *m/z* 711 and 737 are assumed
193 to be formed by the heterocyclic ring fission and retro Diels–Alder cleavage of the
194 catechin unit of the trimer oxide,[17, 18] while quinone-methide cleavage of the interflavan
195 bond generates the fragment ion at *m/z* 287. The fragment ion at *m/z* 693 is produced by
196 the loss of molecular water from the ion corresponding to *m/z* 711; these peaks are also

observed by the MS/MS of **4** prior to oxidation. On the other hand, *m/z* 575, 455, and 449 correspond to product peaks, and are newly observed in the MS/MS spectrum of the *m/z* 863 ion. The fragment ion peak at *m/z* 575 corresponds to the product of catechin-dimer oxidation. Some of the fragment ion peaks (*m/z* 125, 167, 287, 407, and 449) are also observed in the MS/MS spectrum of compound **5**. These results suggest that products exhibiting peaks at *m/z* 863 have spiro-type skeletons, such as **5**, as partial structures in their molecular frameworks. The possibility exists that one of the *m/z* 863-peak products is A-type procyanidin formed through an additional C2-O-C7 ether bond. The transformations of B-type procyanidins to the A-type under alkaline/H_2O_2,[19] DPPH (2,2-diphenyl-1-picrylhydrazyl)-radical,[20] and enzymatic conditions,[21] have been previously reported. Although these oxidation reactions are similar to those used in our experiments, we believe that the A-type structure is not formed in our experiments due to steric factors. The C4 position of the catechin trimer prepared from (+)-catechin mainly exists in the α form. Procyanidin C2, which is α-configured at the C4 position, is produced as the major product through condensation reactions from (+)-catechin. In practice, the α/β ratio at the C4 position was observed to be 7/3 by NMR spectroscopy. Condensed (+)-catechin in the α form is incapable of forming the C2-O-C7 ether bond; therefore, we conclude that A-type structures are hardly produced in this study.

MS/MS of the *m/z* 861 $[M-H]^-$ peak, with a retention time 8.2 min, reveals peaks at *m/z* 407, 453, and 709, which are related to the fragment peaks observed in the MS/MS spectrum of the *m/z* 863 ion. Although the presence of two spiro skeletons in the molecule is assumed on the basis of the peak at *m/z* 861, the expected fragment peaks corresponding to the catechin unit (*m/z* 575) and the remaining component (*m/z* 287) were not observed, suggesting that different types of intramolecular bonds were generated in this case.

Thiolysis degradation reactions. Thiolysis is a known method for the analysis procyanidins. In this method, procyanidins are fragmented into their constituent units in the presence of a thiol, such as thiophenol or 2-mercaptoethanol. Although thiolysis can release the extension unit-thiol adducts and the terminal units from procyanidin B-type polymers, which contain C4–C8 or C4–C6 bonds, this method does not degrade procyanidins possessing other types of bond. We assume that the C4–C8/6 bond in **4** are cleaved by this reaction; however, the new bonds produced by the oxidation of **4** cannot be cleaved; consequently, any novel unit is retained, which facilitates the elucidation of the novel bonding pattern produced through oxidation. Hence, compound **4** and its oxidation mixtures were treated with 2-mercaptoethanol and the reaction solution was subjected to HPLC. Due to thiolytic degradation, the

originally observed peaks were replaced by new peaks, with negative UPLC-ESI-MS of the generated peaks exhibiting pseudo-molecular-ion peaks at *m/z* 575, 651, and 653 $[M-H]^-$.

The thiolysis degradation products were next subjected to UPLC-ESI-MS/MS (Fig. 5). The precursor ion peak at *m/z* 575 corresponds to **5**, which is the oxidation product of procyanidin B3. The *m/z* 575 peak exhibited major fragment ions at *m/z* 449 and 287, which are in agreement with the fragment pattern of **5**. Fragment ions that are 78 Da less than the precursor ions were observed at *m/z* 651 and 653. The loss of 78 Da suggests the presence of the mercaptoethanol residue in these molecules, and these compounds are presumed to be derived from the extended units of **4** or its oxidized product, rather than the terminal unit.[6] The *m/z* 651 peak exhibited major fragment ions at *m/z* 573, 449, and 285; this fragment pattern is similar (each 2 Da less) to that of **5**. Based on this result, the peak with the *m/z* 651 precursor ion is assigned to be the mercaptoethanol adduct of **5**.

Fragment ions from the precursor ion peak at *m/z* 653 were observed at *m/z* 575, 449, and 287, which is same fragment pattern observed for **5**. The spiro ring system formed through the oxidation reaction retains the C4-C6/8 bond; hence we propose that the precursor ion peak at *m/z* 653 is produced by the ring-opening reaction

of the spiro ring system following the formation of the thiol adduct (Fig. S10). These results suggested that the product formed by the oxidation of procyanidin C2 contains a spiro ring system as a main partial structure.

Determining the structure of peak k. As detailed above, the UPLC-MS spectrum of the oxidation mixture of **4** exhibited peaks that increased and decreased in intensity depending on the duration of oxidation (Fig. 3). This is especially evident for peak **k**, with a retention time of 8 min, which was most intense at 0.5 h and decreased in intensity thereafter. The molecular weight corresponding to peak **k** was determined to be 864 Da from the mass chromatogram (2 Da less than that of **4**), suggesting that intramolecular bonds are formed during oxidation, as was observed for **5** (the oxidation product of **3**). Considering the time required to generate peak **k**, we assume that the reaction and bond formation occur in a manner similar to that of compound **5**. In other words, the chemical structure corresponding to peak **k** is presumed to contain the same spiro skeleton as in compound **5**. Therefore, we postulate that peak **k** corresponds to structure **6**, which is obtained through the condensation of the dimer oxide **5** and **2** (Fig. 6). Hence, we separately condensed **5** with **2** and subjected the resulting mixture to HPLC. The retention time of **6** matched that of peak **k**. UPLC-MS of this synthesized trimer revealed a pseudo-molecular ion peak at *m/z* 863 for $[M-H]^-$, which is the same

as that observed for peak **k**. In addition, the MS/MS data are in good agreement with those of peak **k** (Fig. S11). On the basis of these result, **6** was confirmed as the chemical structure corresponding to peak **k**.

As described above, although various peaks were observed in the oxidation mixture in this LC-MS study, their molecular ion peaks were observed at either m/z 861 $[M-H]^-$ or 863 $[M-H]^-$, some of which are possibly stereo- or positional isomers of **6**. In particular, spiro-type compounds, such as **5**, and their derivatives were identified in red rice extracts through thiolysis reactions and HPLC-MS/MS multiple reaction monitoring (MRM) analyses in our previous study.[6] These results reveal that the color deepening in red rice proceeds through the oxidative formation of intramolecular bonds in procyanidins. In contrast, the UV absorptions of compound **6** and other oxidants are insufficient to explanation the color deepening of red rice (Fig. 5). We believe that the internal bonding system formed in procyanidin is one of factors that causes color deepening, but additional other mechanisms might also operate. Further studies are needed in order to clarify and fully understand this phenomenon.

The term "oxidation" is often used to describe the degradation of food quality. It is possible that the UV absorption changes and oxidation products clarified in this study serve as the basis for evaluating the freshness of red rice. In addition, this study will aid

in the further elucidation of the color-deepening phenomenon of red rice as well as various plants containing procyanidins.

ABBREVIATIONS

ESI-MS, electrospray ionization mass spectroscopy; HPLC, high-performance liquid chromatography; NMR, nuclear magnetic resonance; TIC, total ion chromatogram; UPLC, ultra-high-performance liquid chromatography; MRM, multiple reaction monitoring

ACKNOWLEDGMENTS

We thank Dr. Yoshihiro Miwa (Professor Emeritus at Gifu University) for providing the red rice samples, and Dr. Tohru Mitsunaga (Professor at Gifu University) for technical assistance in the preparation of the taxifolin sample.

Supporting Information: Dimer oxidation product structures; additional UV, HPLC, LC/MS, and MS/MS data for mixtures of oxidation products. Supporting Information is available free of charge on the ACS Publications website.

REFERENCES

(1) Chen, M. H.; Choi, S. H.; Kozukue, N.; Kim, H. J.; Friedman, M. Growth-inhibitory effects of pigmented rice bran extracts and three red bran fractions against human cancer cells: Relationships with composition and antioxidative activities. *J. Agric. Food Chem.* **2012**, *60*, 9151-9161.

(2) Itani, T.; Tatemoto, H.; Okamoto, M.; Fujii, K.; Muto, N. A comparative study on antioxidative activity and polyphenol content of colored kernel rice. *J. Jpn. Soc. Food Sci*. **2002**, *49*, 540-543.

(3) Min, B.; McClung, AM.; Chen, MH. Phytochemicals and antioxidant capacities in rice brans of different color. *J. Food Sci*. **2011**, *76*, C117-C126.

(4) Oki, T.; Masuda, M.; Kobayashi, M.; Nishiba, Y.; Furuta, S.; Suda, I.; Sato, T. Polymeric procyanidins as radical-scavenging components in red-hulled rice. *J. Agric. Food Chem.* **2002**, *50*, 7524-7529.

(5) Hayashi, S.; Yanase, E. A study on the color deepening in red rice during storage. *Food Chem.* **2016**, *199*, 457-462.

(6) Hayashi, S.; Kohei, N.; Yanase, E. Investigation of color-deepening phenomenon in catechin - (4 → 8) - dimer as a proanthocyanidin model and structural determination of its derivatives by oxidation. *Food Chem*. **2018**, *239*, 1126-1133.

(7) Mitsunaga, T.; Abe, I.; Kontani, M.; Ono, H.; Tanaka, T. Inhibitory effects of bark proanthocyanidins on the activities of glucosyltransferases of Streptococcus sobrinus. *J. Wood. Chem. Tech.* **1997**, 17, 323-340.

(8) Delcour, J. A.; Ferreira, D.; Roux, D. G. Synthesis of condensed tannins. Part 9. The condensation sequence of leucocyanidin with (+)-catechin and with the resultant procyanidins. *J. Chem. Soc. Perkin Trans. 1* **1983**, *0*, 1711-1717.

(9) Tanaka, T.; Takahashi, R.; Kouno, I.; Nonaka, G. I. Chemical evidence for the de-astringency (insolubilization of tannins) of persimmon fruit. *J. Chem. Soc. Perkin Trans. 1* **1994**, *0*, 3013-3022.

(10) Cédric, D. T.; Marie-Lucie, K. C.; Vesna, J.; Sonia, C. Degradation of (−)-Epicatechin and Procyanidin B2 in Aqueous and Lipidic Model Systems. First Evidence of "Chemical" Flavan-3-ol Oligomers in Processed Cocoa. *J. Agric. Food Chem.*, **2014**, *62*, 9002–9016.

(11) Cédric, D. T.; Marie-Lucie, K. C.; Vesna, J.; Sonia, C. Occurrence and Antioxidant Activity of C1 Degradation Products in Cocoa. *Foods.,* **2017**, *6*, 18.

(12) Ishino, N.; Yanase, E.; Nakatsuka, S. Epimerization of tea catechins under weakly acidic and alkaline conditions. *Biosci. Biotechnol. Biochem*., **2010**, *74*, 875-877.

(13) Callemien, D.; Collin, S. Involvement of Flavanoids in Beer Color Instability during Storage. *J. Agric. Food Chem*., **2007**, 55, 9066-9073.

338 (14) Guyot, S.; Vercauteren, J.; Cheynier, V. Structural determination of colourless
339 and yellow dimers resulting from (+)-catechin coupling catalyzed by grape
340 polyphenoloxidase. *Phytochem*., **1996**, 42, 1279-1288
341 (15) Tanaka, T.; Matsuo, Y.; Kouno, I. Chemistry of Secondary Polyphenols
342 Produced during Processing of Tea and Selected Foods *Int*. *J. Mol. Sci*., **2010,** *11(1)*,
343 14–40
344 (16) Uchida, K.; Ogawa, K.; Yanase, E. Structure Determination of Novel
345 Oxidation Products from Epicatechin: Thearubigin-Like Molecules. *Molecules*,
346 2016, *21 (273)*, 12-14.
347 (17) Hanen, F.; Samia, O.; Sylvain, G.; Alia, B. D.; Christian, M.; Chedly, A.;
348 Riadh, K. LC/ESI-MS/MS characterization of procyanidins and propelargonidins
349 responsible for the strong antioxidant activity of the edible halophyte
350 *Mesembryanthemum edule* L. *Food Chem*. **2011**, *127*, 1732-1738.
351 (18) Gu, L.; Kelm, M. A.; Hammerstone, J. F.; Zhang, Z.; Beecher, G.; Holden, J.;
352 Haytowitz, D.; Prior, R. L. Liquid chromatographic/electrospray ionization mass
353 spectrometric studies of proanthocyanidins in foods. *J. Mass Spectrom*. **2003**, *38*,
354 1272-1280.

355 (19) Morimoto, S.; Nonaka, G.; Nishioka, I. Tannins and Related Compounds.
356 LIX.Aesculitannins, Novel Proanthocyanidins with Doubly-Bonded Structures from
357 Aesculus hippocastanum L. *Chem. Pharm. Bull.* **1987**, 35, 4717-4729.
358 (20) Kondo, K.; Kurihara, M.; Fukuhara, K.; Tanaka, T.;Suzuki, T.; Miyata, N.;
359 Toyoda, M. Conversion of procyanidin B-type (catechin dimer) to A-type: evidence
360 for abstraction of C-2 hydrogen in catechin during radical oxidation. *Tetrahedron*
361 *Lett.* **2000**, 41, 485–488.
362 (21) Osman, A.M.; Wong, K.K.Y. Laccase (EC 1.10.3.2) catalyses the conversion
363 of procyanidin B-2 (epicatechin dimer) to type A-2. *Tetrahedron Lett.* **2007**, 48,
364 1163–1167.

FUNDING SOURCE

This work was partially supported by the Tojuro Iijima Foundation for Food Science and Technology (Chiba, Japan).

368 **FIGURE CAPTIONS**

369 **Figure 1** Chemical structures of catechin (**1**), taxifolin (**2**), procyanidin B3 (**3**),

370 procyanidin C2 (**4**), and oxidized procyanidin B3 (**5**)

371 **Figure 2** UV spectra of procyanidin B3 and procyanidin C2 after oxidation for various

372 times: (A) compound **3** (procyanidin B3), (B) compound **4** (procyanidin C2), and (C)

373 UV absorptions at 330 nm as functions of time. Values are expressed as means with

374 standard error bars (n=3).

375 **Figure 3** Relative contents of compounds **3** and **4** during oxidation as functions of time.

376 **Figure 4** UPLC/MS traces of the mixtures obtained following the oxidation of

377 procyanidin C2 (**4**) for: A) 0.5 h and B) 4 h.

378 **Figure 5** UPLC-MS/MS spectra of thiolysis degradation products: (A) *m/z* 575, (B) *m/z*

379 653, and (C) *m/z* 651.

380 **Figure 6** Proposed structure of **6** (peak **k**) and its fragmentations as determined by

381 MS/MS.

382

Figure 1

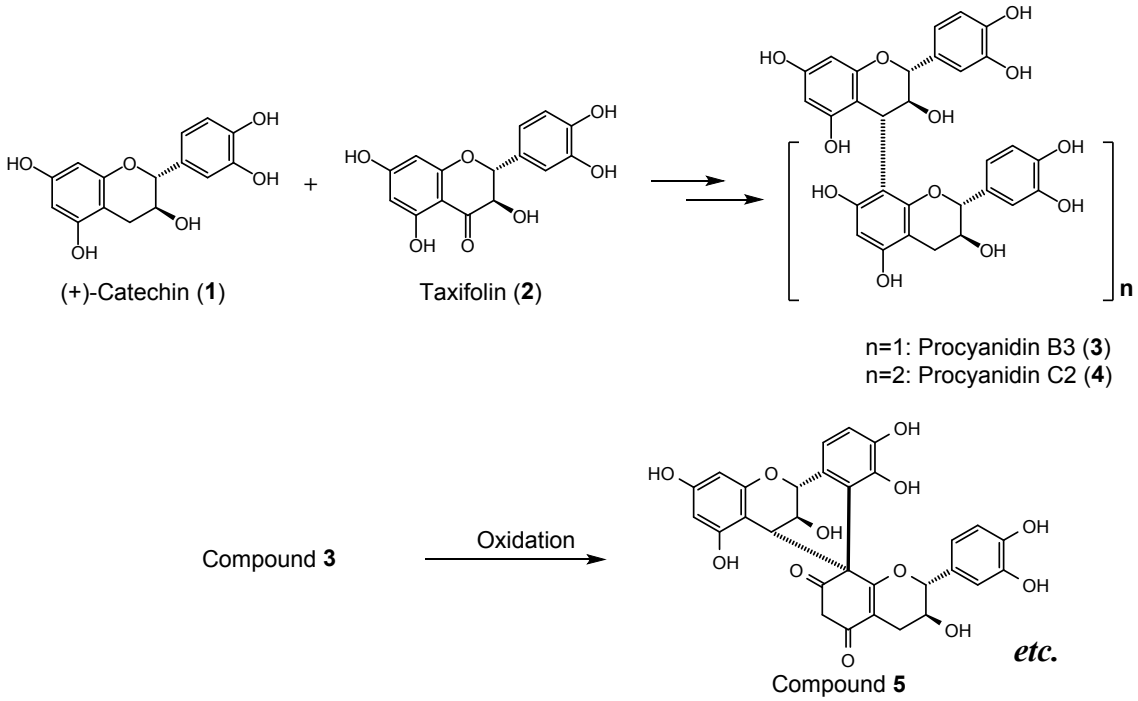
(+)-Catechin (1)
Taxifolin (2)
n=1: Procyanidin B3 (3)
n=2: Procyanidin C2 (4)
Compound 3
Oxidation
Compound 5
etc.

Figure 2

(A)

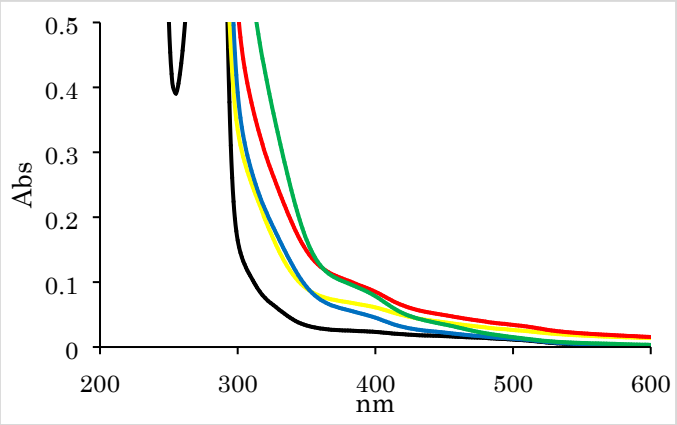
0.5
0.4
0.3
0.2
0.1
0
Abs
200
300
400
500
600
nm

(B)

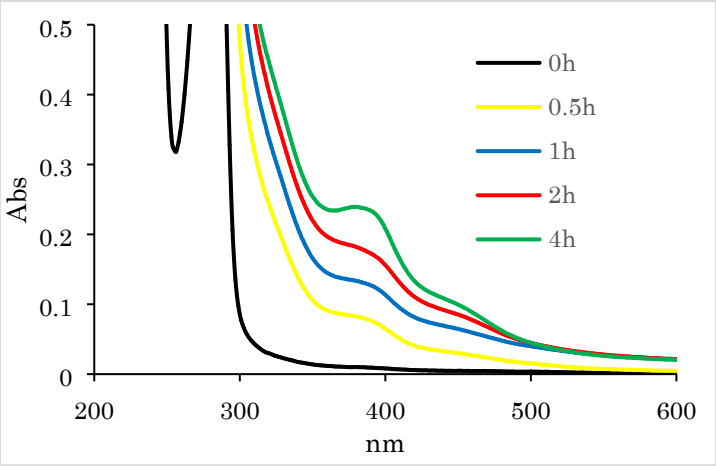
0.5
0.4
0.3
0.2
0.1
0
Abs
200
300
400
500
600
nm
0h
0.5h
1h
2h
4h

(C)

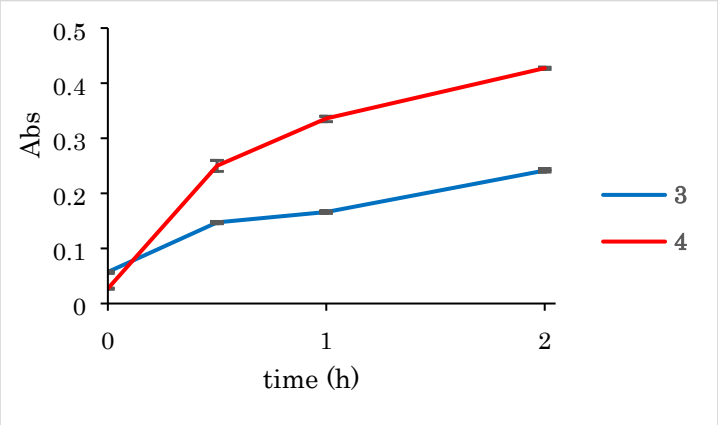
0.5
0.4
0.3
0.2
0.1
0
Abs
0
1
2
time (h)
3
4

Figure 3

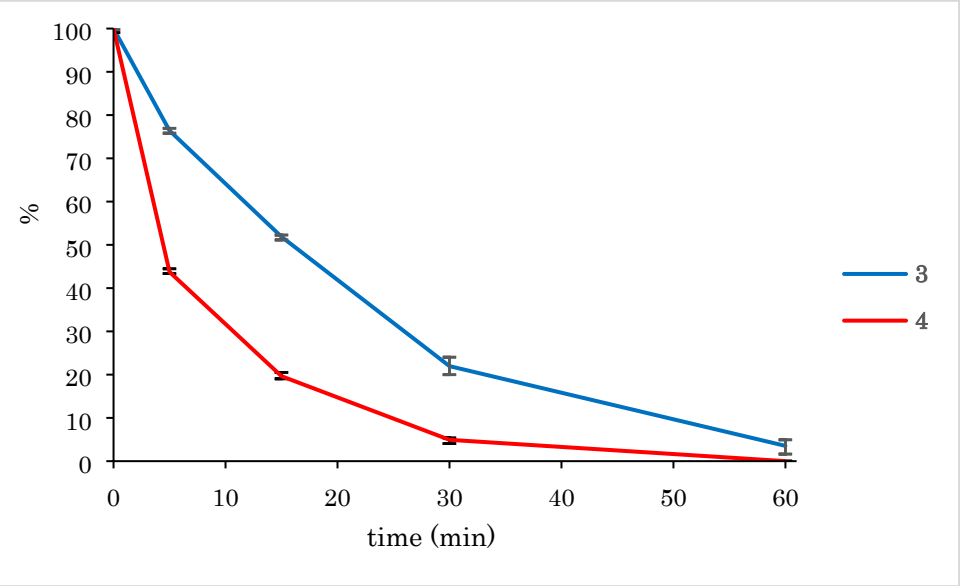

Figure 4

(A)

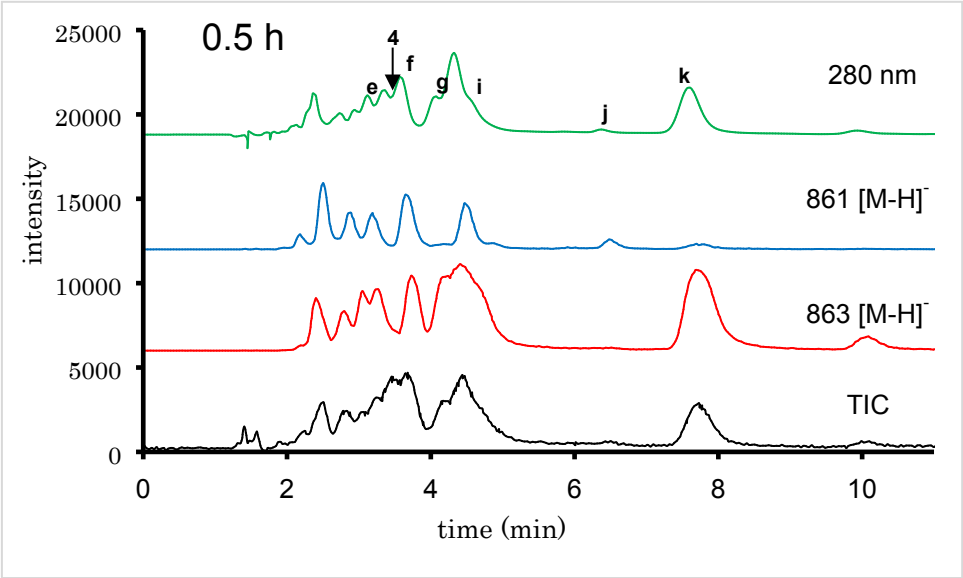
0.5 h
4
f
e
g
i
j
k
280 nm
861 [M-H]-
863 [M-H]-
TIC
intensity
25000
20000
15000
10000
5000
0
0
2
4
6
8
10
time (min)

(B)

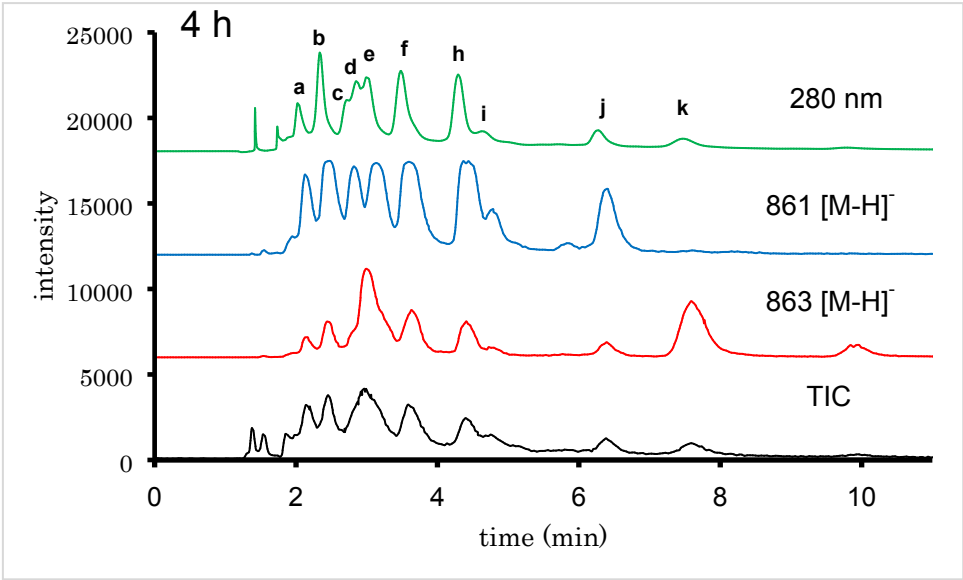
4 h
a
b
c
d
e
f
h
i
j
k
280 nm
861 [M-H]-
863 [M-H]-
TIC
intensity
25000
20000
15000
10000
5000
0
0
2
4
6
8
10
time (min)

Figure 5

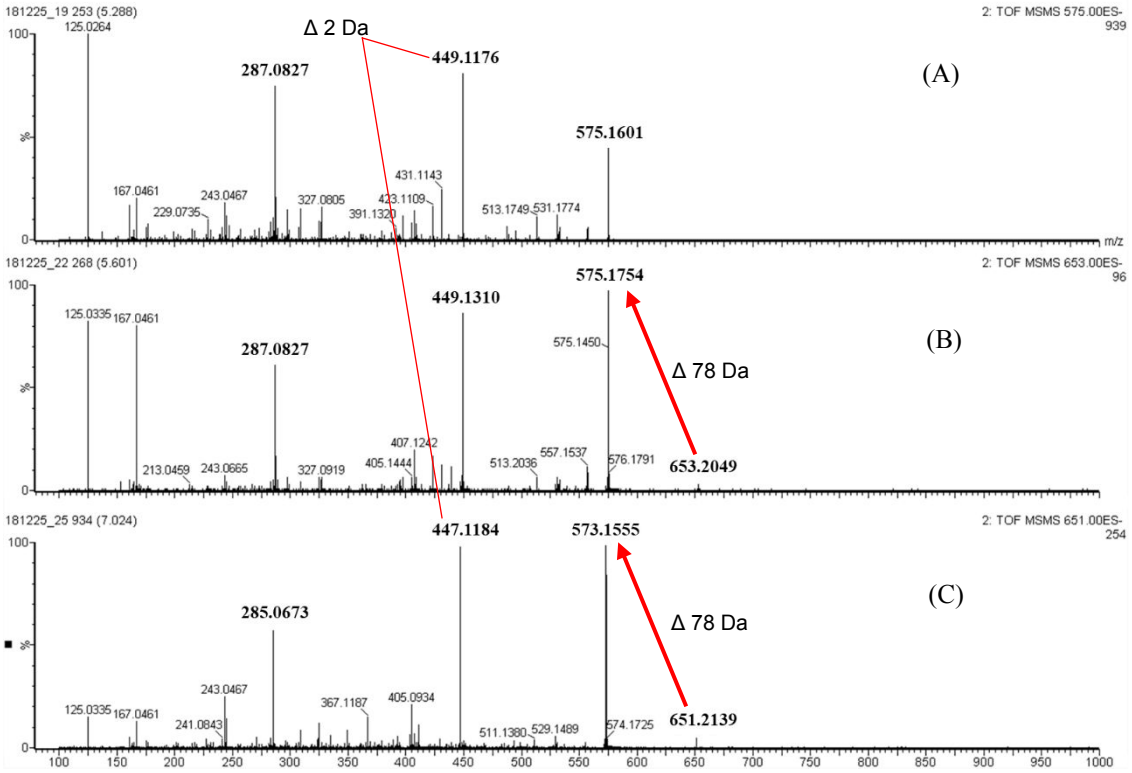
181225_19 253 (5.288)
2: TOF MSMS 575.00ES-939
Δ 2 Da
449.1176
287.0827
575.1601
(A)
181225_22 268 (5.601)
2: TOF MSMS 653.00ES-96
575.1754
449.1310
287.0827
Δ 78 Da
653.2049
(B)
181225_25 934 (7.024)
2: TOF MSMS 651.00ES-254
447.1184
573.1555
285.0673
Δ 78 Da
651.2139
(C)
m/z

Figure 6

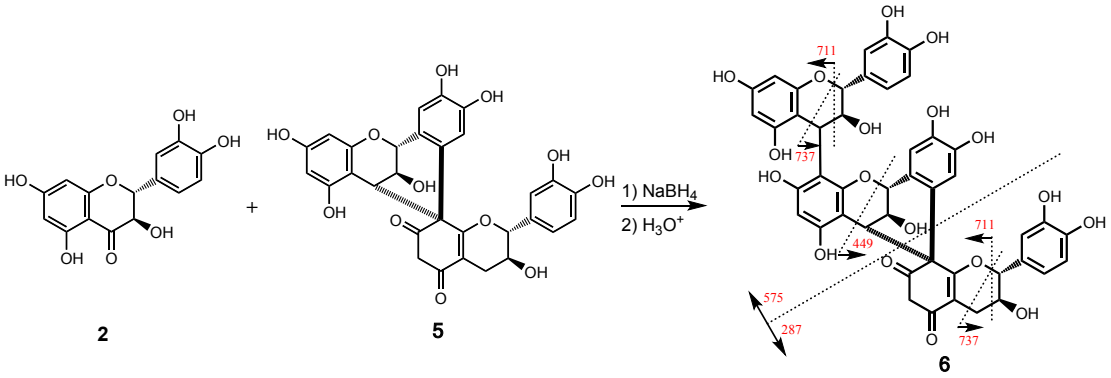

Table of Contents graphic